

Effects of ozone-vegetation coupling on surface ozone air quality via biogeochemical and meteorological feedbacks

Mehliyar Sadiq¹, Amos P. K. Tai^{1,2}, Danica Lombardozzi³, and Maria Val Martin⁴

¹Graduate Division of Earth and Atmospheric Sciences, Faculty of Science, The Chinese University of Hong Kong, Hong Kong

²Earth System Science Programme, Faculty of Science, The Chinese University of Hong Kong, Hong Kong

³National Center for Atmospheric Research, Boulder, Colorado, USA

⁴Department of Chemical and Biological Engineering, University of Sheffield, Sheffield, UK

Correspondence to: Amos P. K. Tai (amostai@cuhk.edu.hk)

Abstract. Tropospheric ozone is one of the most hazardous air pollutants as it harms both human health and plant productivity. Foliage uptake of ozone via dry deposition damages photosynthesis and causes stomatal closure. These foliage changes could lead to a cascade of biogeochemical and biogeophysical effects that not only modulate the carbon cycle, regional hydrometeorology and climate, but also cause feedbacks onto surface ozone concentration itself. In this study, we implement a semi-empirical parameterization of ozone damage on vegetation in the Community Earth System Model to enable online ozone-vegetation coupling, so that for the first time ecosystem structure and ozone concentration can coevolve in fully coupled land-atmosphere simulations. With ozone-vegetation coupling, present-day surface ozone is simulated to be higher by up to 4-6 ppbv over Europe, North America and China. Reduced dry deposition velocity following ozone damage contributes to ~40-100% of those increases, constituting a significant positive biogeochemical feedback on ozone air quality. Enhanced biogenic isoprene emission is found to contribute to most of the remaining increases, and is driven mainly by higher vegetation temperature that results from lower transpiration rate. This isoprene-driven pathway represents an indirect, positive meteorological feedback. The reduction in both dry deposition and transpiration is mostly associated with reduced stomatal conductance following ozone damage, whereas the modification of photosynthesis and further changes in ecosystem productivity are found to play a smaller role in contributing to the ozone-vegetation feedbacks. Our results highlight the need to consider two-way ozone-vegetation coupling in Earth system models to derive a more complete understanding and yield more reliable future predictions of ozone air quality.

1 Introduction

Tropospheric ozone is one of the air pollutants of the greatest concern due to its significant harm to human respiratory health. Increases of ozone since the preindustrial time have been associated with a global annual burden of 0.7 ± 0.3 million respiratory mortalities (Anenberg et al., 2010). Decades of observational records have also demonstrated the damaging effect of surface ozone on vegetation and crop productivity (Ainsworth et al., 2012). The phytotoxicity of ozone is shown to induce stomatal closure and reduce primary production, with ramifications for climate through the modification of surface energy and water fluxes and a decrease in the land carbon sink (Sitch et al., 2007; Wittig et al., 2007; Lombardozzi et al., 2015). Meanwhile, vegetation helps reduce ambient ozone concentration through stomatal deposition (e.g., Kroeger et al., 2014).

39 However, the effect of such ozone-induced vegetation damage on ozone concentration itself, which thereby
40 completes the ozone-vegetation feedback loop, has not been examined before but is potentially significant in
41 modulating tropospheric ozone. This work uses a fully coupled land-atmosphere model to, for the first time,
42 quantify the impacts of ozone-vegetation coupling on surface ozone, and diagnoses the contributions from
43 various feedback pathways in terrestrial ecosystems.

44 Tropospheric ozone is mainly produced from the photochemical oxidation of carbon monoxide (CO),
45 methane (CH₄) and non-methane volatile organic compounds (VOCs) by hydroxyl radical (OH) in the presence
46 of nitrogen oxides (NO_x ≡ NO + NO₂). Vegetation plays various significant roles modulating surface ozone
47 concentration. Precursor gases of ozone have large anthropogenic and natural sources, including vegetation and
48 soil microbes for CH₄ and other VOCs. The most abundant single non-methane VOC species emitted by
49 vegetation is isoprene (C₅H₈), which acts as a major precursor for ozone formation in polluted, high-NO_x
50 regions, but eliminates ozone by direct ozonolysis or by sequestering NO_x as isoprene nitrate in more pristine
51 environments (Fiore et al., 2011). The major sinks for tropospheric ozone include photolysis in the presence of
52 water vapor and uptake by vegetation (i.e., dry deposition, mainly through the leaf stomata). Vegetation,
53 therefore, plays a significant role in modulating ozone biogeochemically through dry deposition and biogenic
54 VOC emissions. Meanwhile, transpiration from vegetation can affect ozone by regulating the overlying
55 hydrometeorological environment. For instance, transpiration influences near-surface water vapor content,
56 which affects the chemical loss rate of ozone. Transpiration also controls surface temperature and mixing depth,
57 which can all influence the formation and dilution of ozone in the atmospheric boundary layer (Jacob and
58 Winner, 2009).

59 Vegetation not only affects but is also affected by surface ozone. Stomatal uptake of ozone by leaves
60 damages internal plant tissues, leading to severe damage to forest, grassland and agricultural productivity
61 (Ashmore, 2005; Karnosky et al., 2007; Ainsworth et al., 2012). Elevated ozone since the industrial revolution is
62 suggested to have reduced light-saturated photosynthetic rate and stomatal conductance by 11% and 13%,
63 respectively (Wittig et al., 2007). Modeling studies have also suggested that elevated ozone could decrease gross
64 primary production (GPP) by 4-8% in the eastern US and more severely so (11-17%) in several hot spots there
65 (Yue and Unger, 2014), and decrease transpiration rate globally by 2-2.4% (Lombardozzi et al., 2015), with
66 significant implications for climate. For instance, the ozone-induced reduction in the global land carbon sink by
67 2100 is shown to have an indirect radiative forcing of +0.62-1.09 W m⁻², which is comparable to the direct
68 radiative forcing of ozone as a greenhouse gas (0.89 W m⁻²) and contributes to more pronounced warming (Sitch
69 et al., 2007). Changes in stomatal conductance also modify the land-atmosphere exchange of water and energy
70 and thus regional hydrometeorology (Bernacchi et al., 2011; Lombardozzi et al., 2015). In view of the important
71 roles vegetation plays in shaping tropospheric ozone, the above biogeochemical and biogeophysical effects
72 induced by ozone damage would affect not only weather and climate but also constitute important feedbacks
73 that ultimately affect ozone air quality itself.

74 In many land surface models, photosynthetic rate and stomatal conductance are highly coupled through
75 the computation within the Farquhar/Ball-Berry model (Farquhar et al., 1980; Ball et al., 1987; Bonan et al.,
76 2011). In global modeling studies on ozone-mediated vegetation changes and climate (Sitch et al., 2007; Collins
77 et al., 2010; Yue and Unger, 2014), the effects of ozone damage on photosynthesis and stomata are thus strongly
78 coupled to each other. Ozone uptake is assumed to directly affect photosynthetic rate, which in turn affects

stomatal conductance via changes in internal CO₂ concentration. However, recent studies have suggested that separate modification of photosynthetic rate and stomatal conductance by cumulative ozone uptake in the Community Land Model (CLM) leads to better representation of plant responses to ozone exposure (Lombardozzi et al., 2012). This decoupling of ozone effects on photosynthesis and stomata is shown to decrease water use efficiency of affected plants, but leads to an overall smaller impact of ozone on transpiration and GPP than previously predicted.

Many climate-chemistry-biosphere modeling studies performed to date have demonstrated the importance of the coevolution of climate, land cover and terrestrial ecosystems in air quality simulations and predictions (Wu et al., 2012; Tai et al., 2013; Pacifico et al., 2015), but they have not taken into account the potentially strong feedbacks arising from ozone damage on vegetation. For instance, ozone exposure can reduce stomatal conductance and thus transpiration rate, which may modify the partition between latent and sensible heat fluxes and lead to a cascade of meteorological changes: lower humidity that reduces the chemical loss rate of ozone; a thicker boundary layer that dilutes all pollutants, but may enhance entrainment, which either increases or decreases surface ozone depending on the vertical ozone profile; and higher temperature that enhances ozone mainly through increased biogenic emissions and higher abundance of NO_x (Jacob and Winner, 2009). These transpiration-mediated pathways can be characterized as biogeophysical feedbacks as are commonly known in the context of climate change, but here we prefer to call them hydrometeorological or simply “meteorological feedbacks” to emphasize that they are effected through ozone-induced changes in the hydrometeorological variables that ultimately affect ozone. On the other hand, reduced dry deposition caused by lower stomatal conductance and a possible decline in leaf area index (LAI) following ozone exposure can potentially increase ozone. The short-term impact of ozone on foliage-level isoprene emission is still under debate (Fares et al., 2006; Calfapietra et al., 2007), but as foliage density (e.g., represented by LAI) declines due to chronic ozone exposure (Yue et al., 2014), isoprene emission would likely decrease in the long term. These pathways directly involving plant biogeochemistry and atmospheric chemistry can be collectively termed “biogeochemical feedbacks”. Fig. 1 summarizes the potentially important biogeochemical and meteorological feedbacks on surface ozone concentration, which are expected to have ramifications for simulations and future projections of ozone air quality. Such feedbacks may further alter atmospheric composition (e.g., aerosol and oxidant concentrations) and climate at large but remain poorly characterized in an Earth system modeling framework.

In this study, we adopt and implement a semi-empirical scheme for ozone-induced vegetation damage (Lombardozzi et al., 2015) into a coupled land-atmosphere model with fully interactive atmospheric chemistry and biogeochemical cycles, and examine the resulting impacts on present-day simulations of tropospheric ozone air quality with respect to observations. We perform sensitivity simulations to quantify the relative importance of different biogeochemical and meteorological feedback pathways, elucidate the larger sources of uncertainties, and make specific suggestions regarding Earth system model development.

2 Methods

2.1 Model description

This study investigates the impacts of ozone-vegetation coupling on ozone concentrations using the Community Earth System Model (CESM), which includes several different model components representing the

atmosphere, land, ocean, and sea ice to be run independently or in various coupled configurations (Oleson et al., 2010; Lamarque et al., 2012; Neale et al., 2013). We employ CESM version 1.2.2 with fully interactive atmosphere and land components, but with prescribed ocean and sea ice consistent with the scenarios of concern. For the atmosphere component, we use the Community Atmosphere Model version 4 (CAM4) (Neale et al., 2013) fully coupled with an atmospheric chemistry scheme (i.e., CAM-Chem) that contains full tropospheric O₃-NO_x-CO-VOC-aerosol chemistry based on the MOZART-4 chemical transport model (CTM) (Emmons et al., 2010; Lamarque et al., 2012). The version of CAM-Chem simulates the concentrations of 56 atmospheric chemical species at a horizontal resolution of 1.9°×2.5° latitude-longitude and 26 vertical layers for the atmosphere up to around 40 km.

For the land component, we use the Community Land Model version 4 (CLM4) (Oleson et al., 2010) with active carbon-nitrogen biogeochemistry (CLM4CN), which contains prognostic treatment of terrestrial carbon and nitrogen cycles (Lawrence et al., 2011). In CLM4, the Model of Emissions of Gases and Aerosols from Nature (MEGAN) version 2.1 is used to compute biogenic emissions online as functions of changing LAI, vegetation temperature, soil moisture and other environmental conditions (Guenther et al., 2012). For dry deposition of gases and aerosols we use the resistance-in-series scheme in CLM4 as described in Lamarque et al. (2012) with a further update of optimized coupling of stomatal resistance to LAI (Val Martin et al., 2014). Evapotranspiration is calculated based on the Monin-Obukhov similarity theory and the diffusive flux-resistance model with dependence on vegetation, ground and surface temperature, specific humidity, and an ensemble of resistances that are functions of meteorological and land surface conditions (Oleson et al., 2010; Lawrence et al., 2011; Bonan et al., 2011). Evapotranspiration is partitioned into transpiration, ground evaporation and canopy evaporation, with updates from Lawrence et al. (2011), and is linked to photosynthesis via the computation of stomatal resistance, as described below.

2.2 Photosynthesis- stomatal conductance model and ozone damage parameterization

The Farquhar/Ball-Berry model is used in CLM4CN to compute leaf-level photosynthetic rate and stomatal conductance under different environmental conditions (Farquhar et al., 1980; Ball et al., 1987). Leaf photosynthetic rate, A ($\mu\text{mol CO}_2 \text{ m}^{-2} \text{ s}^{-1}$), is calculated as

$$A = \min(W_c, W_j, W_e) \quad (1)$$

where W_c is the Ribulose-1,5-bisphosphate carboxylase (RuBisCO)-limited rate of carboxylation, W_j is the light-limited rate, and W_e is the export-limited rate. Photosynthesis and stomatal conductance (g_s) are related by

$$g_s = \frac{1}{r_s} = m \frac{A e_s}{c_s e_i} P_{\text{atm}} + b \quad (2)$$

where g_s is the leaf stomatal conductance; r_s is the leaf stomatal resistance ($\text{s m}^2 \mu\text{mol}^{-1}$); m is the slope of the conductance-photosynthesis relationship with values ranging from 5 to 9; c_s is the CO₂ partial pressure at leaf surface (Pa); e_s is the vapor pressure at leaf surface (Pa); e_i is the saturation vapor pressure inside the leaf (Pa); P_{atm} is the atmospheric pressure (Pa); and b is the minimum stomatal conductance when $A = 0$, and is set to give a maximum stomatal resistance of 20000 s m^{-1} in CLM4 (Oleson et al., 2010).

Parameterization for the impact of ozone exposure on photosynthesis and stomatal conductance follows the work of Lombardozzi et al., (2015), who tested the sensitivity of global ecosystem productivity and hydrometeorology to ozone damage on vegetation using satellite phenology (i.e., prescribed LAI, canopy height, etc.) and present-day ozone concentrations. The scheme uses two sets of ozone impact factors, one for

modifying photosynthetic rate and another for stomatal conductance independently. These factors account for different plant groups, and are calculated based on the [cumulative uptake of ozone \(CUO\)](#) under different levels of chronic ozone exposure (Lombardozzi et al., 2013). CUO integrates ozone flux into leaves over the growing season as

$$CUO = \sum(k_{O_3}/r_s) [O_3] \quad (3)$$

where $[O_3]$ is the surface ozone concentration computed from CAM-Chem at every time step (30 minutes), and k_{O_3} is the ratio of leaf resistance to ozone to leaf resistance to water. Ozone uptake is only cumulated during the growing season when vegetation is most vulnerable to air pollution episodes; growing season is defined as the period in which total leaf area index (TLAI) > 0.5 (Lombardozzi et al., 2012). Ozone uptake only cumulates when the ozone flux is above a critical threshold, $0.8 \text{ nmol } O_3 \text{ m}^{-2} \text{ s}^{-1}$, to account for ozone detoxification by vegetation at lower ozone levels (Lombardozzi et al., 2015). Three different plant groups are accounted for: evergreen, deciduous, and crops/grasses. The ozone impact factors have empirical linear relationships with CUO such that

$$F_{pO_3} = a_p \times CUO + b_p \quad (4)$$

$$F_{cO_3} = a_c \times CUO + b_c \quad (5)$$

where F_{pO_3} is the ozone damage factor multiplied to the photosynthesis rate (A), and a_p and b_p are slope and intercept from empirical and experimental studies (listed in Table 1); F_{cO_3} is the ozone damage factor multiplied to stomatal conductance (g_s), and a_c and b_c are the corresponding slope and intercept (Table 1). The ozone damage is applied to the optimal photosynthesis and stomatal conductance values, which are calculated iteratively first without ozone damage, to allow the damage to be applied independently.

2.3 Model experiments

Incorporating the ozone-vegetation parameterization above into CLM4CN and coupling it with CAM-Chem, we allow, for the first time, ecosystem structure (e.g., in terms of LAI and canopy height) to evolve in response to ozone exposure but at the same time allow ozone concentration to evolve in response to such ecosystem changes. Therefore, online ozone-vegetation coupling and feedback are included. We conduct four sets of fully coupled land-atmosphere simulations: 1) a control case without ozone damage on vegetation ([CTR]); 2) simulation with both photosynthetic rate and stomatal conductance modified by ozone impact factors (independently) ([PHT+COND]), following the approach of Lombardozzi et al (2015); 3) simulation where we apply the ozone impact factor to photosynthetic rate only ([PHT]), but stomatal conductance is calculated using the intact, optimal photosynthetic rate; and 4) simulation where we apply the ozone impact factor to stomatal conductance only ([COND]), but photosynthetic rate is calculated using the intact stomatal conductance. Simulations [PHT] and [COND], when compared with [PHT+COND], allow us to quantify the relative contribution from each pathway. To determine the relative contribution of those pathways involving biogenic emissions toward the overall ozone-vegetation feedback, we conduct an additional set of sensitivity simulations with prescribed isoprene emission and MEGAN turned off: a control case with no MEGAN

(CTR_nM), and a simulation with modified photosynthesis and stomatal conductance but with no MEGAN ([PHT+COND_nM]). To determine the relative contribution of pathways involving dry deposition vs. transpiration, we compare simulated results with that of Val Martin et al. (2014) who have used the similar CAM-Chem-CLM framework but without ozone-vegetation coupling to test the sensitivity of ozone to perturbations in dry deposition velocity.

All simulations are conducted for 20 years using year 2000 initial conditions and the corresponding land cover data (e.g., land cover and land use types, satellite LAI, etc.). The first five years of outputs are treated as spin-up and thus discarded in the analysis. We observe that the annual averages of key aboveground ecosystem parameters such as LAI and ozone concentration come into a relatively steady state after 5 years. We focus on changes in the 15-year northern summertime (JJA) averages for most of the variables in the rest of this paper because this is the period when the growing season of the majority of global vegetation overlaps most significantly with high-ozone season especially in the northern midlatitudes.

3 Simulated ozone with and without ozone-vegetation coupling

Figure 2 shows the 15-year mean summertime surface ozone concentration from the [PHT+COND] simulation. The corresponding cumulative uptake of ozone (CUO) used to affect vegetation is shown in supplemental Fig. S1. Simulated ozone is generally higher in the northern midlatitudes than elsewhere, and is the highest over the Mediterranean where solar radiation is particularly strong. CUO also has high values in Europe, but the overall distribution does not exactly follow that of surface ozone concentration because CUO also depends on the length of the growing season and stomatal conductance. CUO ranges between 20-70 mmol m⁻² over regions with both high summertime ozone and high productivity. The simulated CUO is comparable in both magnitude and spatial distribution with Lombardozzi et al., (2015), who used prescribed meteorology, ozone and vegetation phenology with no active carbon-nitrogen cycle or atmospheric coupling, as opposed to this study. This suggests that online ozone-vegetation coupling, which can modify ozone concentration substantially depending on the region, lead to a similar pattern of ozone damage on vegetation to the case using prescribed ozone. During the growing season, CUO is used to calculate the ozone impact factors that modify photosynthetic rate and stomatal conductance according to Eq. (4) and (5) and parameter values listed in Table 1.

Figure 3 shows the differences in surface ozone concentration in different simulations from the control case (corresponding relative changes shown in supplemental Fig. S2). Implementing ozone-vegetation coupling that includes simultaneous modification of photosynthetic rate and stomatal conductance by ozone exposure (the [PHT+COND] case) increases mean surface ozone globally, and significant increases by up to 4-6 ppbv are found over China, North America and Europe (Fig. 3a). Ozone exposure is thus found to constitute a positive feedback loop via vegetation that ultimately enhances surface ozone levels when ozone-vegetation coupling is accounted for.

The simulated increases in ozone levels due to ozone-vegetation coupling are significant when compared with the possible impacts of 2000-2050 climate and land cover changes on surface ozone, which are in the range of +1-10 ppbv (Jacob & Winner, 2009; Tai et al., 2013; Val Martin et al., 2015). These simulated increases, however, slightly worsen the performance of CAM-Chem in reproducing ozone concentrations against observations as seen in Fig. 4, which shows the model-observation comparison for the control case

(standard CAM-Chem-CLM with dry deposition improvement of Val Martin et al. (2014)) and the [PHT+COND] case. The high-biases in CESM-simulated summertime surface ozone concentrations in North America and Europe are a commonly acknowledged issue with CAM-Chem (Lamarque et al., 2012) and other global and regional models (Lapina et al., 2014; Parrish et al., 2014). [Uncertain emissions, coarse resolution \(Lamarque et al., 2012\), misrepresentation of dry deposition process and overestimation of stomatal resistance \(Val Martin et al., 2014\) are all likely factors contributing to these high biases.](#) Inclusion of ozone-vegetation coupling in the model further increases the normalized mean biases of the modeled results against three sets of observational data: Clean Air Status and Trends Network (CASTNET) (1999-2001), Air Quality System (AQS) (1999-2001), and European Monitoring and Evaluation Programme (EMEP) (1999-2001), from 18% to 22%, 31% to 35%, 14% to 22%, respectively. [Although there remains considerable uncertainty in the parameterization of ozone-vegetation coupling and in ozone simulations by Earth system models, we show that including ozone damage in a coupled climate-chemistry-biosphere framework can have a potentially significant impact on surface ozone simulations.](#)

4 Attribution to different biogeochemical and meteorological feedback pathways

Figures 3(b) and 3(c) show the differences in ozone for the cases where ozone damages stomatal conductance alone and photosynthesis alone, respectively, noting that each of them is calculated using the undamaged, intact values of the other variable. Comparison of Fig. 3(a) with (b)-(c) shows that the modification of stomatal conductance by ozone uptake contributes more dominantly to the overall effect of ozone-vegetation coupling (Fig. 3a). This suggests that, among the various feedback pathways that may influence surface ozone (Fig. 1), those triggered by changes in stomatal conductance are generally more important than those associated with photosynthesis or the associated changes in ecosystem production and structure including LAI, at least in the modeling framework of this study. This is also supported by sensitivity simulations performed under the same modeling framework but without ozone damage, in which a 50% of increase in LAI decreases summertime surface ozone by on average 3 ppb, which is relatively small in comparison with the changes following optimization of stomatal resistance (Val Martin et al., 2014). Indeed, the effect of modifying stomatal conductance alone ([COND]; Fig. 3b) is slightly larger than the case of [PHT+COND] (Fig. 3a), where the additional effect of modifying photosynthesis together with stomatal conductance would slightly offset the overall positive feedback on ozone. It is noteworthy that this additional effect is, however, not consistent with the effect of modifying photosynthesis alone ([PHT]; Fig. 3c), reflecting nonlinear interactions between photosynthesis and stomatal conductance.

Figure 5 shows the differences in dry deposition velocity, transpiration rate and biogenic isoprene emission between the [PHT+COND] and [CTR] simulations ([relative changes shown in supplemental Fig. S3](#)). Over China, Europe and North America, ozone dry deposition velocity is lower (by up to ~20%) in [PHT+COND]. In these same regions but especially in the eastern US, southern Europe and southern China, isoprene emission is significantly higher (by up to ~50%). In addition, in similar regions but especially in central North America, the transpiration rate is reduced by ozone exposure (by up to ~20%), which would reduce boundary-layer humidity, increase surface temperature, enhance dry convection and thicken the boundary layer. In view of Fig. 1, all of these pathways may add to or offset each other, leading to the overall ozone changes seen in Fig. 3(a). The sensitivity simulations and comparison with Val Martin et al. (2014), which

examined the sensitivity of simulated ozone to differences in dry deposition schemes under essentially the same modeling framework, allow us to quantify more precisely which of these pathways are more important as we discuss next.

Figure 6(a) shows the changes in surface ozone in the [PHT+COND_nM] minus CTR_nM simulations, where we use prescribed biogenic emissions from the original control case (CTR) to drive ozone chemistry so that we essentially shut down any feedback pathways involving biogenic emissions. A comparison between Fig. 6(a) and Fig. 3(a) shows that the changes in biogenic isoprene emissions account for ~0-60% of the ozone increases over Europe, North America and China, while dry deposition and/or transpiration-driven meteorological changes (excluding the temperature effect on isoprene emission) account for remaining ~40-100%. We further show in Fig. 6(b) the theoretical changes in surface ozone by multiplying the dry deposition changes in Fig. 5(a) by the change in ozone concentration per unit change in dry deposition velocity from the study of Val Martin et al. (2014), which provided the sensitivity of simulated ozone to perturbed dry deposition only without the complication of stomatal coupling with hydrometeorology. We find that the ozone changes in Fig. 6(a) and Fig. 6(b) are similar in magnitude, suggesting that globally most of the non-isoprene-driven differences in ozone is driven by dry deposition. Notable exceptions include the US Midwest and southeastern Europe, where higher mixing depth following reduced transpiration might have partly offset the ozone positive feedback; and western Europe, where the lower chemical loss rate following reduced transpired water might have further enhanced the positive feedback.

The simulated general reduction in dry deposition velocity and transpiration rate (Fig. 5a and 5b) is mostly due to increased stomatal resistance (Fig. 7a), i.e., reduced stomatal conductance, a direct response to cumulative uptake of ozone. The reduced dry deposition represents a positive biogeochemical feedback on ozone (orange arrows in Fig. 1). The simulated increase in biogenic isoprene emission (Fig. 5c) is found to be mostly driven by higher surface (thus vegetation) temperature (Fig. 7b) that results from lower transpiration rate and latent heat flux (Fig. 7c). Therefore, this feedback loop involving biogenic emissions is indeed an indirect, meteorological feedback that is also initiated by stomatal and transpiration changes (purple arrows in Fig. 1). Relative changes in variables shown in Fig. 7 are included in supplemental Fig. S4.

By including immediate ozone-vegetation coupling, we find a larger decline in transpiration rate (6.4% globally) than in the offline, uncoupled land model results (2.0-2.4%) estimated by Lombardozzi et al. (2015). On the other hand, although reduced photosynthesis and the resulting long-term changes in GPP and LAI (Fig. 7d-e) play a smaller role than reduced stomatal conductance in shaping simulated ozone (Fig. 3b-c), the impacts are not negligible (up to 3 ppb), especially as these changes are also nonlinearly coupled to stomatal changes. Photosynthetic rate decreases by up to 20% directly due to the ozone effect (Fig. 7f), which is quite similar both in magnitude and spatial pattern to the results of Lombardozzi et al. (2015), but the corresponding GPP and LAI changes are relatively small (~5% over regions concerned, except for Southeast Asia, where the highest ozone-induced LAI reduction is simulated and leads to isoprene emission decrease despite higher surface temperature). Grid-level GPP and LAI in certain areas increase despite reduced leaf-level photosynthetic rate, likely reflecting more carbon allocation to leaves to compensate the reduced photosynthetic rate and relaxation of resource limitation as nutrients and water become less limiting upon lower photosynthetic and evaporative demands, as well as favorable hydrometeorological changes following reduced transpiration (e.g., enhanced vegetation temperature, precipitation and soil moisture). These LAI increases induced by ozone are not represented in Fig.

1 because they more likely reflect the fully coupled effect of changing hydrometeorology, instead of the direct effect of ozone on LAI as is typically observed in experimental studies (Ainsworth et al., 2012).

5 Conclusions and discussion

Tropospheric ozone is one the most hazardous air pollutants due to its harmful effects on human health and damage to forest and agricultural productivity. Stomatal uptake of ozone by leaves reduces both photosynthetic rate and stomatal conductance. These vegetation changes can induce a cascade of biogeochemical and biogeophysical (or meteorological) effects (Fig. 1) that ultimately modulate climate, carbon cycle and also feedback onto ozone air quality itself. The direct, biogeochemical feedback pathways include reduced ozone dry deposition and biogenic VOC emissions. The indirect, meteorological feedback pathways are facilitated by transpiration-driven changes in the meteorological environment that influence ozone formation and removal. A few land surface modeling studies have estimated the direct effects of ozone on ecosystem production and land-atmosphere water exchange (Yue and Unger, 2014; Lombardozzi et al., 2015), and predicted a possible positive radiative forcing from the ozone-induced decline in the land-carbon sink (Sitch et al., 2007).

In this study, we implement a semi-empirical parameterization of ozone damage on vegetation (Lombardozzi et al., 2015) into the CESM (CAM4-Chem-CLM4CN) modeling framework to enable online ozone-vegetation coupling so that vegetation variables can evolve in response to ozone exposure, and at the same time simulated ozone concentration can respond to ecosystem changes. Our scheme modifies leaf-level photosynthesis and stomatal conductance separately via the ozone impact factors, which are assumed to have empirical linear relationships with cumulative uptake of ozone and account for different plant groups. Sensitivity simulations are conducted to determine the relative importance of different feedback pathways.

With ozone-vegetation coupling, surface ozone is simulated to be higher by up to 4-6 ppbv over Europe, North America and China. This coupling effect is significant in view of the 2000-2050 effects of climate and land cover changes on surface ozone (+1-10 ppbv) as found in previous work (Jacob and Winner, 2009; Tai et al., 2013), and should be considered in future air quality projection studies. Reduced dry deposition velocity following the modification contributes to ~40-100% and enhanced biogenic isoprene emission contributes to ~0-60% of the higher ozone concentrations. The dry deposition-driven ozone increases (by up to 4 ppbv) arise mostly from reduced stomatal conductance, and are consistent with the sensitivity of ozone to perturbations in dry deposition velocity found by Val Martin et al. (2014). This pathway constitutes a significant positive biogeochemical feedback on surface ozone. The other major feedback associated with enhanced isoprene emission is mostly driven by higher vegetation temperature that results from lower transpiration rate. This pathway constitutes an indirect, positive meteorological feedback on surface ozone. Depending on the region, transpiration-driven meteorological changes such as lower humidity and deeper mixing depth may also influence surface ozone. Transpiration rate is simulated to decrease by 6.4% globally, which is a larger change compared with the decrease estimated by Lombardozzi et al. (2015), who used prescribed instead of synchronously simulated atmospheric forcings. This also suggests an augmented effect on transpiration due to changes in foliage density, surface temperature and ozone concentration arising from ozone-vegetation feedbacks.

Modification of photosynthesis and further long-term changes in ecosystem productivity and structure, including LAI changes, are found to play a smaller role in contributing to the ozone-vegetation feedbacks than direct stomatal changes, but are not insignificant (up to +3 ppbv). The simulated changes in LAI (less than 5%) in this study are similar in magnitude to that by Yue et al. (2015), who included an active carbon cycle though using Yale Interactive terrestrial Biosphere (YIBs) model with a different ozone-vegetation parameterization. However, prognostic treatment of the carbon cycle and LAI calculation in CLM4CN are still known to be problematic, with large uncertainties and biases in the estimation of global carbon fluxes (Sun et al., 2012), arising from incomplete model parameterization and from uncertainty in photosynthetic parameters (Bonan et al., 2011). It is not surprising that changes in GPP as simulated here do not replicate the results of Lombardozzi et al. (2015), in which vegetation phenology is prescribed and the carbon and nitrogen cycles are not active (CLM4.5SP). Implementing ozone damage on vegetation in a model with more sophisticated and realistic representation of prognostic carbon-nitrogen cycle is highly warranted, so that the possible effects of ozone-induced long-term ecosystem changes can be examined more fully.

Large variability in the responses of different plants to ozone leads to considerable uncertainties in any global-scale studies (Lombardozzi et al., 2013). Such large variability in plant responses across different studies, in some cases, weakens the correlation between phytotoxic responses and CUO. Such correlation is usually more evident in individual studies, and in the parametrization schemes based on them (Sitch et al., 2007; Yue et al., 2014). The parameterization developed by Lombardozzi et al. (2013), based on the most comprehensive database available for photosynthetic and stomatal responses to CUO to date, is deemed more appropriate for the global scale of this study and the plant functional types represented in the model, despite the weaker correlation between plant responses and CUO as shown by the compilation of data across studies. The damage is applied after CUO reaches a certain threshold, so the calculation of CUO is still crucial to the application of the damage functions. The model results could possibly be improved with more detailed plant-type-specific ozone damage parameterization, including better estimates of plant vulnerability to ozone that will help refine the ozone uptake thresholds (Lombardozzi et al., 2015). An important caveat of this study is the consideration of only three plant groups to generalize the responses of global vegetation to ozone exposure because data are largely unavailable for other plant groups.

Another potential caveat is the uncertainty and lack of cross-validation in hydrometeorological simulations with respect to the ozone phytotoxicity scheme we newly implement, as we only focus on vegetation and atmospheric chemical changes in this study. Although most simulated vegetation variables are consistent with previous work, the changes in simulated vegetation temperature from ozone-vegetation coupling are not small (by up to +2°C) (Fig. 7b) and they result in quite substantial changes in isoprene emission, suggesting the need for further tuning of hydrometeorological processes in the model. Also, MEGAN does not consider the direct, immediate biochemical connection between photosynthesis and biogenic emissions, by which ozone damage on photosynthesis may directly reduce isoprene emission and partially offset the significant temperature-induced increase in isoprene emission as shown in Fig. 5c (Tiwari et al., 2015). Whereas the various environmental activity factors used in MEGAN to adjust baseline emissions may have implicitly encapsulated the biochemical connection with photosynthesis, further incorporating such connection into ozone-vegetation modeling warrants more in-depth investigation. In general, we have the highest confidence in the quantification of the biogeochemical pathway via stomata-driven deposition changes, which is straightforward

and accounts for the majority of the ozone-vegetation feedbacks. On the other hand, the hydrometeorological feedbacks introduce strong nonlinearity in the interactions between atmospheric chemistry and vegetation that is more difficult to isolate and understand. Parameterizing the ozone-vegetation coupling in a standalone chemical transport model with prescribed meteorology could be particularly helpful to more confidently separate between the effects of biogeochemical vs. meteorological feedbacks. This knowledge will be important in projecting the impacts of future climate and land cover changes on ozone air quality and climate feedbacks in the coming decades.

Acknowledgment

This work was supported by the Early Career Scheme (Project Number: 24300614) of the Research Grants Council of Hong Kong, and the associated Direct Grant for Research (Project ID: 4441337, 3132767) from The Chinese University of Hong Kong (CUHK), given to the principal investigator, Amos P. K. Tai. We also thank the Information Technology Services Centre (ITSC) at CUHK for their devotion in providing the necessary computational services for this work.

References

- Ainsworth, E. A., Yendrek, C. R., Sitch, S., Collins, W. J., and Emberson, L. D.: The Effects of Tropospheric Ozone on Net Primary Productivity and Implications for Climate Change, *Annu Rev Plant Biol*, 63, 637-661, doi: 10.1146/annurev-arplant-042110-103829, 2012.
- Anenberg, S. C., Horowitz, L. W., Tong, D. Q., and West, J. J.: An Estimate of the Global Burden of Anthropogenic Ozone and Fine Particulate Matter on Premature Human Mortality Using Atmospheric Modeling, *Environ Health Persp*, 118, 1189-1195, doi:10.1289/ehp.0901220, 2010.
- Ashmore, M. R.: Assessing the future global impacts of ozone on vegetation, *Plant Cell Environ*, 28, 949-964, doi:10.1111/J.1365-3040.2005.01341.X, 2005.
- Ball, J. T., Woodrow, I. E., and Berry, J. A.: A model predicting stomatal conductance and its contribution to the control of photosynthesis under different environmental conditions, *Prog. Photosynthesis*, 221-224, 1987.
- Bernacchi, C. J., Leakey, A. D. B., Kimball, B. A., and Ort, D. R.: Growth of soybean at future tropospheric ozone concentrations decreases canopy evapotranspiration and soil water depletion, *Environ Pollut*, 159, 1464-1472, doi:10.1016/j.envpol.2011.03.011, 2011.
- Bonan, G. B.: Forests and climate change: Forcings, feedbacks, and the climate benefits of forests, *Science*, 320, 1444-1449, doi:10.1126/science.1155121, 2008.
- Bonan, G. B., Lawrence, P. J., Oleson, K. W., Levis, S., Jung, M., Reichstein, M., Lawrence, D. M., and Swenson, S. C.: Improving canopy processes in the Community Land Model version 4 (CLM4) using global flux fields empirically inferred from FLUXNET data, *J Geophys Res-Bioge*, 116, G02014, doi:10.1029/2010jg001593, 2011.
- Calfapietra, C., Wiberley, A. E., Falbel, T. G., Linskey, A. R., Mugnozza, G. S., Karnosky, D. F., Loreto, F., and Sharkey, T. D.: Isoprene synthase expression and protein levels are reduced under elevated O₃ but not under elevated CO₂ (FACE) in field-grown aspen trees, *Plant Cell Environ*, 30, 654-661, doi:10.1111/j.1365-3040.2007.01646.x, 2007.

433 Collins, W. J., Sitch, S., and Boucher, O.: How vegetation impacts affect climate metrics for ozone precursors, *J*
434 *Geophys Res-Atmos*, 115, D23308, doi:10.1029/2010jd014187, 2010.

435 Emmons, L. K., Walters, S., Hess, P. G., Lamarque, J. F., Pfister, G. G., Fillmore, D., Granier, C., Guenther, A.,
436 Kinnison, D., Laepple, T., Orlando, J., Tie, X., Tyndall, G., Wiedinmyer, C., Baughcum, S. L., and Kloster, S.:
437 Description and evaluation of the Model for Ozone and Related chemical Tracers, version 4 (MOZART-4),
438 *Geosci Model Dev*, 3, 43-67, 2010.

439 Fares, S., Barta, C., Brilli, F., Centritto, M., Ederli, L., Ferranti, F., Pasqualini, S., Reale, L., Tricoli, D., and
440 Loreto, F.: Impact of high ozone on isoprene emission, photosynthesis and histology of developing *Populus alba*
441 leaves directly or indirectly exposed to the pollutant, *Physiol Plantarum*, 128, 456-465, doi: 10.1111/j.1399-
442 3054.2006.00750.x, 2006.

443 Farquhar, G. D., Caemmerer, S. V., and Berry, J. A.: A Biochemical-Model of Photosynthetic Co₂ Assimilation
444 in Leaves of C-3 Species, *Planta*, 149, 78-90, doi:10.1007/Bf00386231, 1980.

445 Fiore, A. M., Levy, H., and Jaffe, D. A.: North American isoprene influence on intercontinental ozone pollution,
446 *Atmos Chem Phys*, 11, 1697-1710, doi:10.5194/acp-11-1697-2011, 2011.

447 Gauss, M., Myhre, G., Pitari, G., Prather, M. J., Isaksen, I. S. A., Bernsten, T. K., Brasseur, G. P., Dentener, F. J.,
448 Derwent, R. G., Hauglustaine, D. A., Horowitz, L. W., Jacob, D. J., Johnson, M., Law, K. S., Mickley, L. J.,
449 Muller, J. F., Plantevin, P. H., Pyle, J. A., Rogers, H. L., Stevenson, D. S., Sundet, J. K., van Weele, M., and
450 Wild, O.: Radiative forcing in the 21st century due to ozone changes in the troposphere and the lower
451 stratosphere, *J Geophys Res-Atmos*, 108, 4292, doi:10.1029/2002jd002624, 2003.

452 Guenther, A. B., Jiang, X., Heald, C. L., Sakulyanontvittaya, T., Duhl, T., Emmons, L. K., and Wang, X.: The
453 Model of Emissions of Gases and Aerosols from Nature version 2.1 (MEGAN2.1): an extended and updated
454 framework for modeling biogenic emissions, *Geosci Model Dev*, 5, 1471-1492, doi:10.5194/gmd-5-1471-2012,
455 2012.

456 Herbinger, K., Then, C., Haberer, K., Alexou, M., Low, M., Remele, K., Rennenberg, H., Matyssek, R., Grill,
457 D., Wieser, G., and Tausz, M.: Gas exchange and antioxidative compounds in young beech trees under free-air
458 ozone exposure and comparisons to adult trees, *Plant Biol*, 9, 288-297, doi:10.1055/s-2006-924660, 2007.

459 Jacob, D. J. and Winner, D. A.: Effect of climate change on air quality, *Atmos Environ*, 43(1), 51-63,
460 doi:10.1016/j.atmosenv.2008.09.051, 2009.

461 Karnosky, D. F., Skelly, J. M., Percy, K. E., and Chappelka, A. H.: Perspectives regarding 50 years of research
462 on effects of tropospheric ozone air pollution on US forests, *Environ Pollut*, 147, 489-506,
463 doi:10.1016/j.envpol.2006.08.043, 2007.

464 Kroeger, T., Escobedo, F. J., Hernandez, J. L., Varela, S., Delphin, S., Fisher, J. R., & Waldron, J.: Reforestation
465 as a novel abatement and compliance measure for ground-level ozone, *P Natl A Sci*, 111(40), E4204-E4213,
466 doi:10.1073/pnas.1409785111, 2014.

467 Lamarque, J. F., Emmons, L. K., Hess, P. G., Kinnison, D. E., Tilmes, S., Vitt, F., Heald, C. L., Holland, E. A.,
468 Lauritzen, P. H., Neu, J., Orlando, J. J., Rasch, P. J., and Tyndall, G. K.: CAM-chem: description and evaluation
469 of interactive atmospheric chemistry in the Community Earth System Model, *Geosci Model Dev*, 5, 369-411,
470 doi:10.5194/gmd-5-369-2012, 2012.

471 Lapina, K., Henze, D. K., Milford, J. B., Huang, M., Lin, M., Fiore, A. M., Carmichael, G., Pfister, G. G., and
 472 Bowman, K.: Assessment of source contributions to seasonal vegetative exposure to ozone in the US, *J Geophys*
 473 *Res-Atmos*, 119(1), 324-340, doi: 10.1002/2013JD020905, 2014.
 474 Lawrence, D. M., Oleson, K. W., Flanner, M. G., Thornton, P. E., Swenson, S. C., Lawrence, P. J., Zeng, X. B.,
 475 Yang, Z. L., Levis, S., Sakaguchi, K., Bonan, G. B., and Slater, A. G.: Parameterization Improvements and
 476 Functional and Structural Advances in Version 4 of the Community Land Model, *J Adv Model Earth Sy*, 3,
 477 M03001, doi:10.1029/2011ms000045, 2011.
 478 Lombardozzi, D., Sparks, J. P., Bonan, G., and Levis, S.: Ozone exposure causes a decoupling of conductance
 479 and photosynthesis: implications for the Ball-Berry stomatal conductance model, *Oecologia*, 169, 651-659,
 480 doi:10.1007/s00442-011-2242-3, 2012.
 481 Lombardozzi, D., Sparks, J. P., and Bonan, G.: Integrating O₃ influences on terrestrial processes: photosynthetic
 482 and stomatal response data available for regional and global modeling, *Biogeosciences*, 10, 6815-6831,
 483 doi:10.5194/bg-10-6815-2013, 2013.
 484 Lombardozzi, D., Levis, S., Bonan, G., Hess, P. G., and Sparks, J. P.: The Influence of Chronic Ozone Exposure
 485 on Global Carbon and Water Cycles, *J Climate*, 28, 292-305, doi:10.1175/JCLI-D-14-00223.1, 2015.
 486 Marenco, A., Gouget, H., Nedelec, P., Pages, J. P., and Karcher, F.: Evidence of a Long-Term Increase in
 487 Tropospheric Ozone from Pic Du Midi Data Series - Consequences - Positive Radiative Forcing, *J Geophys*
 488 *Res-Atmos*, 99, 16617-16632, doi:10.1029/94jd00021, 1994.
 489 Neale, R. B., Richter, J., Park, S., Lauritzen, P. H., Vavrus, S. J., Rasch, P. J., and Zhang, M. H.: The Mean
 490 Climate of the Community Atmosphere Model (CAM4) in Forced SST and Fully Coupled Experiments, *J*
 491 *Climate*, 26, 5150-5168, doi:10.1175/JCLI-D-12-00236.1, 2013.
 492 Oleson, K. W., Lawrence, D. M., Gordon, B., Flanner, M. G., Kluzek, E., Peter, J., Levis, S., Swenson, S. C.,
 493 Thornton, E., and Feddema, J.: Technical description of version 4.0 of the Community Land Model (CLM),
 494 2010.
 495 Pacifico, F., Folberth, G. A., Sitch, S., Haywood, J. M., Rizzo, L. V., Malavelle, F. F., and Artaxo, P.: Biomass
 496 burning related ozone damage on vegetation over the Amazon forest: a model sensitivity study, *Atmos Chem*
 497 *Phys*, 15, 2791-2804, doi:10.5194/acp-15-2791-2015, 2015.
 498 Parrish, D. D., Lamarque, J. F., Naik, V., Horowitz, L., Shindell, D. T., Staehelin, J., Derwent, R., Cooper, O. R.,
 499 Tanimoto, H., Volz-Thomas, A. and Gilge, S.: Long-term changes in lower tropospheric baseline ozone
 500 concentrations: Comparing chemistry-climate models and observations at northern midlatitudes, *J Geophys Res-*
 501 *Atmos*, 119(9), 5719-5736, doi: 10.1002/2013JD021435, 2014.
 502 Sitch, S., Cox, P. M., Collins, W. J., and Huntingford, C.: Indirect radiative forcing of climate change through
 503 ozone effects on the land-carbon sink, *Nature*, 448, 791-U794, doi:10.1038/nature06059, 2007.
 504 Sun, Y., Gu, L. H., and Dickinson, R. E.: A numerical issue in calculating the coupled carbon and water fluxes in
 505 a climate model, *J Geophys Res-Atmos*, 117, D22103, doi:10.1029/2012jd018059, 2012.
 506 Tai, A. P. K., Mickley, L. J., Heald, C. L., and Wu, S. L.: Effect of CO₂ inhibition on biogenic isoprene emission:
 507 Implications for air quality under 2000 to 2050 changes in climate, vegetation, and land use, *Geophys Res Lett*,
 508 40, 3479-3483, doi:10.1002/grl.50650, 2013.
 509 Tiwari, S., Grote, R., Churkina, G., Butlet, T.: Ozone damage, detoxification and the role of isoprenoids - new
 510 impetus for integrated models, *Funct Plant Biol*, 43(4) 324-336, 2016.

Val Martin, M., Heald, C. L., and Arnold, S. R.: Coupling dry deposition to vegetation phenology in the Community Earth System Model: Implications for the simulation of surface O₃, *Geophys Res Lett*, 41(8), 2988-2996, doi:10.1002/2014GL059651, 2014.

Val Martin, M., Heald, C. L., Lamarque, J. F., Tilmes, S., Emmons, L. K., and Schichtel, B. A.: How emissions, climate, and land use change will impact mid-century air quality over the United States: a focus on effects at national parks, *Atmos Chem Phys*, 15, 2805-2823, 2015.

Wittig, V. E., Ainsworth, E. A., and Long, S. P.: To what extent do current and projected increases in surface ozone affect photosynthesis and stomatal conductance of trees? A meta-analytic review of the last 3 decades of experiments, *Plant Cell Environ*, 30, 1150-1162, doi:10.1111/j.1365-3040.2007.01717.x, 2007.

Wu, S., Mickley, L. J., Kaplan, J. O., and Jacob, D. J.: Impacts of changes in land use and land cover on atmospheric chemistry and air quality over the 21st century, *Atmos Chem Phys*, 12, 1597-1609, doi:10.5194/acp-12-1597-2012, 2012.

Yue, X., and Unger, N.: Ozone vegetation damage effects on gross primary productivity in the United States, *Atmos Chem Phys*, 14, 9137-9153, doi:10.5194/acp-14-9137-2014, 2014.

Yue, X., and Unger, N.: The Yale Interactive terrestrial Biosphere model version 1.0: description, evaluation and implementation into NASA GISS ModelE2, *Geosci Model Dev*, 8, 2399-2417, doi:10.5194/gmd-8-2399-2015, 2015.

529 Table 1. Slopes (per mmol m^{-2}) and intercepts (unitless) used to calculate ozone impact
 530 factors in Eq. (4) and (5), following Lombardozzi et al. (2015).
 531

Plant group	Photosynthesis		Conductance	
	Slope (a_p)	Intercept (b_p)	Slope (a_c)	Intercept (b_c)
Broadleaf	0	0.8752	0	0.9125
Needleleaf	0	0.839	0.0048	0.7823
Crops and grasses	-0.0009	0.8021	0	0.7511

532

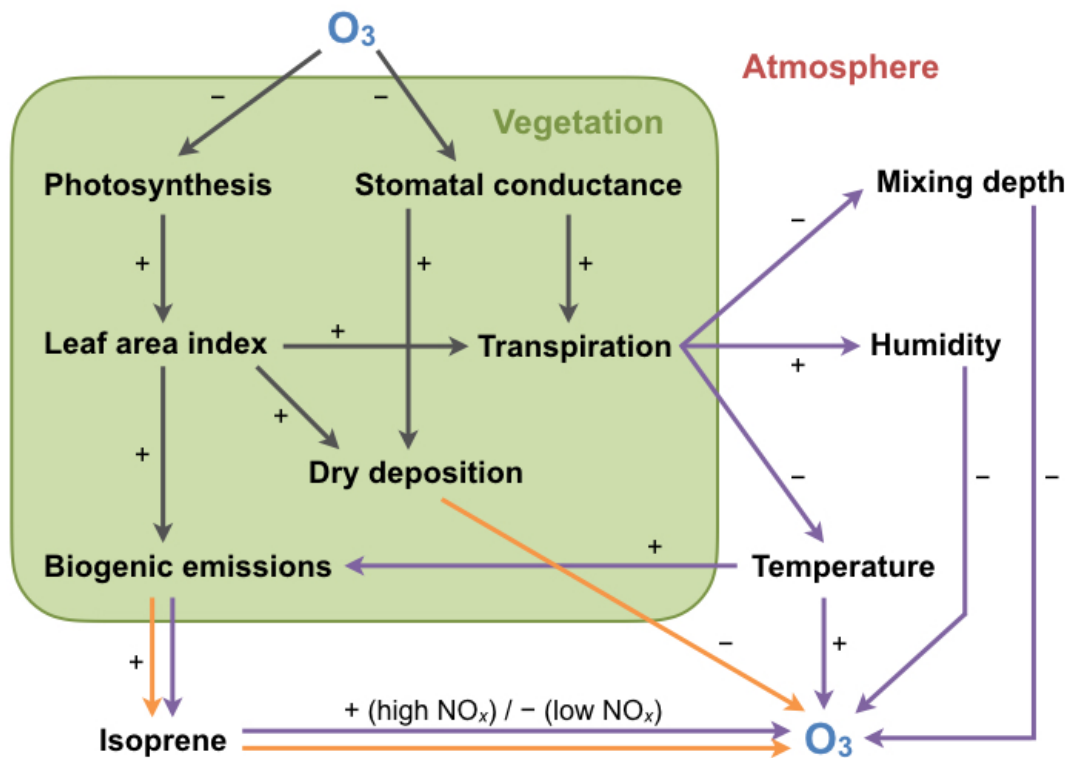


Figure 1. Possible pathways of ozone-vegetation coupling and feedbacks. The sign on each arrow indicates the sign of correlation or effect of one variable with or on another variable; the product of all signs along a given pathway indicates the overall sign of feedback. Orange arrows indicate biogeochemical feedbacks (i.e., via modulating atmospheric chemistry directly); purple arrows indicate meteorological feedbacks (i.e., via modifying the hydrometeorological environment). We focus only on processes that directly affect ozone; meteorological feedbacks on photosynthesis and stomatal conductance are included in the model but not emphasized in this figure.

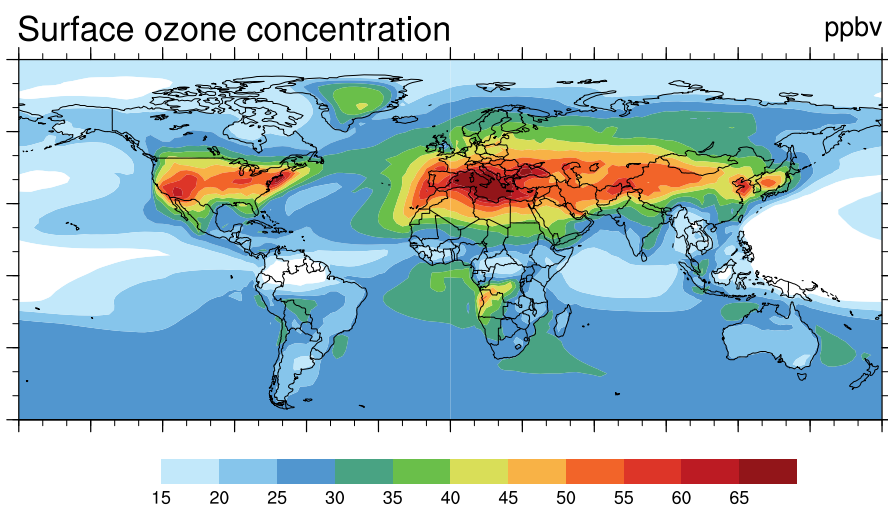


Figure 2. Mean summertime (JJA) surface ozone concentration from the [PHT+COND] case, where ozone uptake simultaneously modifies both photosynthetic rate and stomatal conductance. Results are averaged over the last 15 years of simulations.

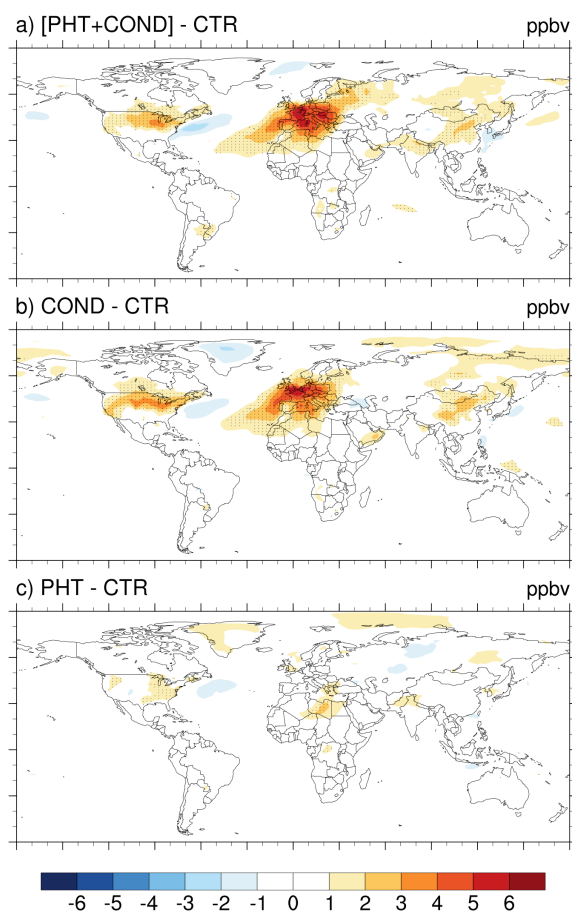


Figure 3. Changes in summertime surface ozone concentrations in different simulations: (a) the case where both photosynthetic rate and stomatal conductance are modified by ozone uptake; (b) modified photosynthetic rate only; and (c) modified stomatal conductance only, all relative to the control case (CTR). Stippling with dots indicates significant changes at 90% confidence from Student's *t* test.

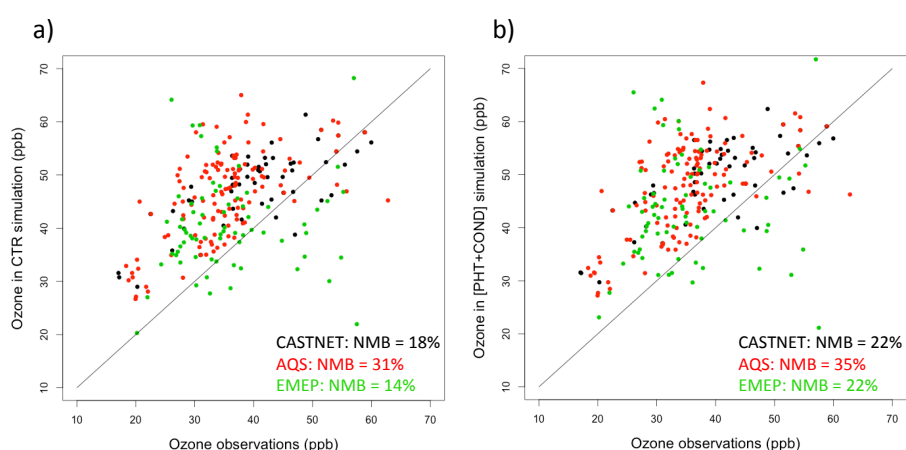


Figure 4. Scatterplots of simulated summertime ozone concentration in (a) the control case (CTR); and (b) the case where both photosynthesis and conductance are modified by ozone uptake ([PHT+COND]), versus observed average values from the Clean Air Status and Trends Network (CASTNET) (1999-2001), Air Quality System (AQS) (1999-2001), and European Monitoring and Evaluation Programme (EMEP) (1999-2001). Normalized mean biases (NMB) are also shown.

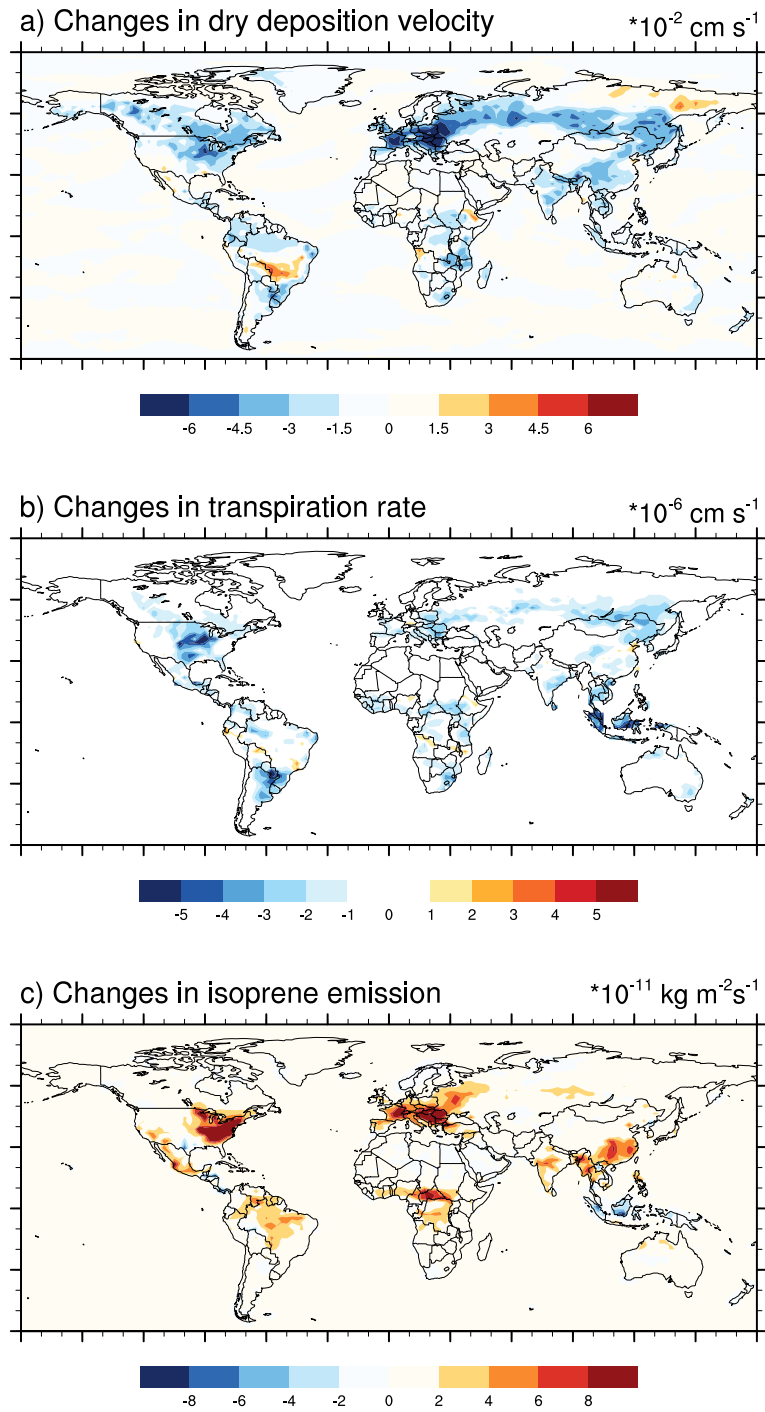


Figure 5. Changes in (a) dry deposition velocity, (b) transpiration rate and (c) isoprene emission in the [PHT+COND] case, where both photosynthetic rate and stomatal conductance are modified by ozone uptake, relative to the control case (CTR).

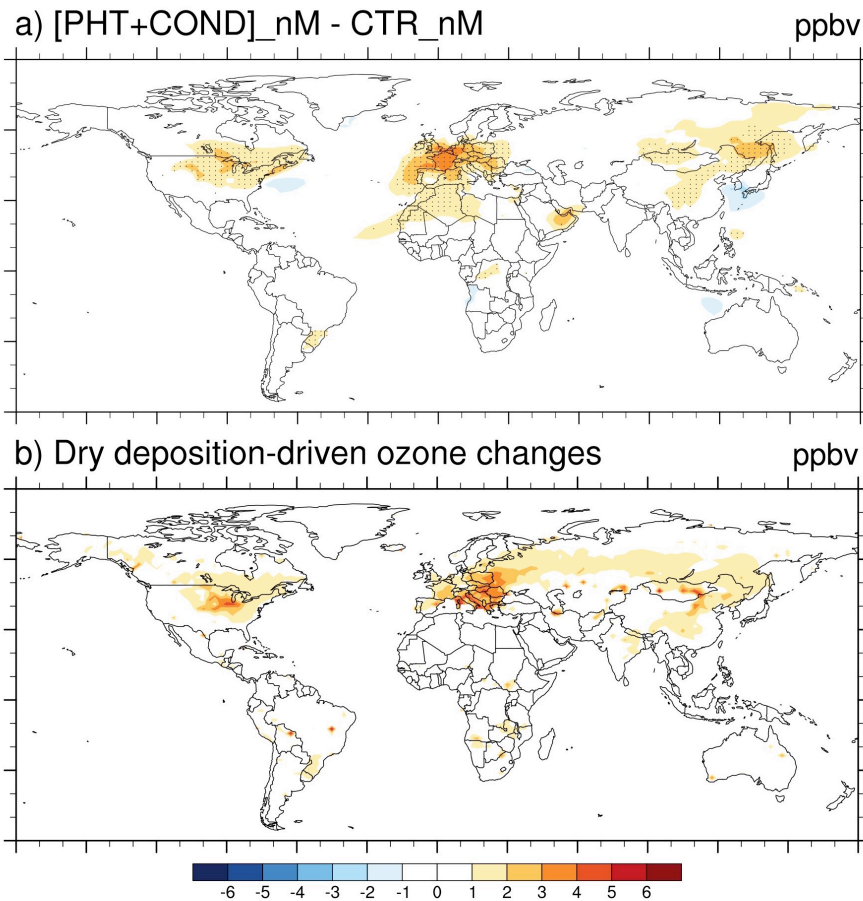
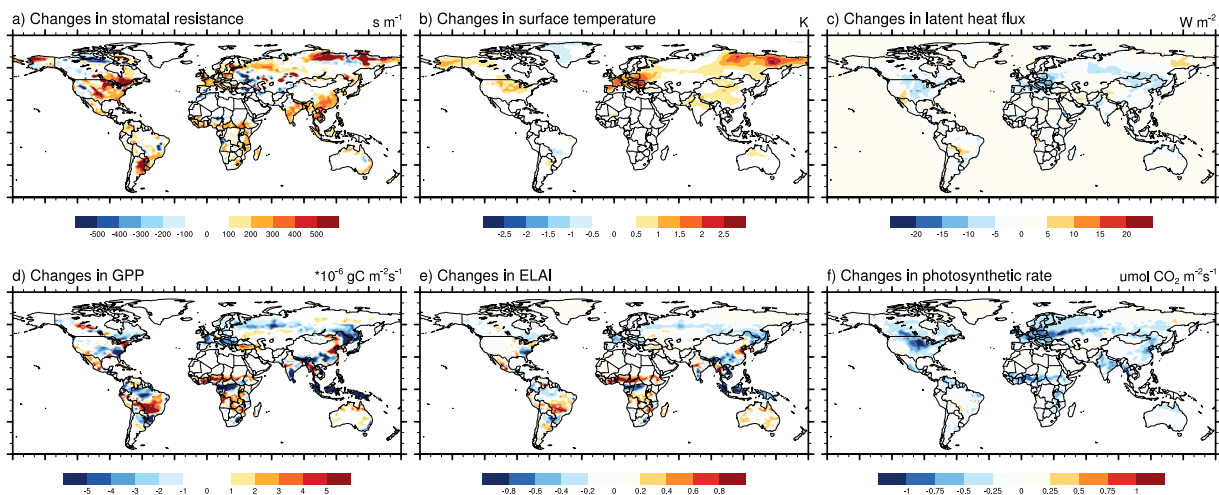


Figure 6. Changes in surface ozone concentration in: (a) the case where both photosynthesis and stomatal conductance are modified by ozone uptake, but with prescribed isoprene emission from the original control case (CTR) by turning off MEGAN (stippling with dots indicates significant changes at 90% confidence from Student's *t* test); and (b) theoretical changes calculated by multiplying our simulated dry deposition changes with the change in ozone concentration per unit change in dry deposition from Val Martin et al. (2014), which did not include ozone damage on vegetation.

566



567

568

569

570

Figure 7. Changes in (a) stomatal resistance, (b) surface temperature, (c) latent heat flux, (d) gross primary production (GPP), (e) effective leaf area index (ELAI) and (f) photosynthetic rate in the [PHT+COND] case, where both photosynthetic rate and stomatal conductance are modified by ozone uptake, relative to the control case (CTR).